

Joint Routing and Control Optimization in VANET

^{1st} Chen Huang
School of Cyber Engineering
Xidian University
Xi'an, China

^{2nd} Dingxuan Wang
School of Cyber Engineering
Xidian University
Xi'an, China

^{3rd} Ronghui Hou
School of Cyber Engineering
Xidian University
Xi'an, China

Abstract—In this paper, we introduce DynaRoute, an adaptive joint optimization framework for dynamic vehicular networks that simultaneously addresses platoon control and data transmission through trajectory-aware routing and safety-constrained vehicle coordination. DynaRoute guarantees continuous vehicle movement via platoon safety control with optimizing transmission paths through real-time trajectory prediction and ensuring reliable data. Our solution achieves three key objectives: (1) maintaining platoon stability through accurate data transmission, (2) enabling adaptive routing based on vehicle movement patterns, and (3) enhancing overall intelligent transportation system performance. DynaRoute equires predefined traffic models and adapts to dynamic network conditions using local vehicle state information. We present comprehensive simulation results demonstrating that DynaRoute maintains control and transmission performance in multiple complex scenarios while significantly improving throughput and reliability compared to traditional approaches.

Index Terms—Vehicle platooning, multi-objective optimization, dynamic routing, model predictive control (MPC)

I. INTRODUCTION

The rapid advancement of Internet of Things (IoT) technology has transformed modern vehicles from simple transportation tools into sophisticated communication hubs. Functioning as both receiving and transmitting nodes, these connected vehicles play a dual role in Intelligent Transportation Systems (ITS). As receivers, they continuously collect real-time environmental data, enabling autonomous trajectory planning and adaptive velocity control through intelligent algorithms, thereby enhancing road throughput and optimizing overall ITS performance. Simultaneously, as transmitters, they leverage roadside infrastructure to deliver essential services including navigation, communication, and entertainment [1].

The high mobility of vehicles leads to rapid topology changes and unstable connections, particularly in congested areas where bandwidth exhaustion leads to packet backlog, preventing real-time transmission and introducing additional latency. The shared wireless channel experiences frequent collisions, further exacerbating performance degradation caused by data transmission delays, with Dedicated Short-Range Communications (DSRC) being especially vulnerable to interference and signal degradation [2], [3]. These dynamics significantly impair IoV communications, safety information delivery and platoon coordination. Traditional routing methods

often were proved inadequate in addressing these mobility-induced challenges [4], highlighting the need for solutions that better accommodate dynamic network conditions while optimizing routing overhead to improve resource utilization in increasingly complex IoT environments.

With the growing demand for intelligent transportation systems, autonomous vehicle operation relies critically on control mechanisms to ensure safe driving. Many works simultaneously consider the communication system and the control system in intelligent vehicular systems. Some works study the impact of communication on control performance to find the appropriate communication parameters [11]–[15]. Other works design the communication schemes to meet the control system requirements [5]–[10]. In this paper, we study the joint optimization of routing and control. In one hand, efficient routing scheme produces smaller packet transmission delay, and then, the control system may obtain more real-time state information to perform a better control. On the other hand, the control system timely feedbacks the controlling decision to help the routing system adapts its routing solution to improve network communication quality. Although a very related work in [16] also jointly considered routing and controlling, the work did not simultaneously optimization both systems but optimized both systems individually. In this paper, we propose DynaRoute—an integrated control-communication optimization framework that constructs mobility-aware link evaluation metrics and accurately predicts vehicle trajectories. Our solution dynamically optimizes transmission routes through real-time node position prediction, ensuring reliable and timely data delivery across diverse traffic conditions while simultaneously improving platoon control performance through enhanced transmission precision. Compared to conventional approaches, the proposed method demonstrates significant improvements in network efficiency and robustness under high-mobility scenarios, while advancing the overall performance of intelligent transportation systems.

II. RELATED WORK

In Vehicular Ad-hoc Network (VANET), inter-vehicle communication is affected by various environmental and nodal factors, which further impact vehicle platoon and overall system performance. Consequently, maintaining ideal inter-vehicle spacing, reducing spacing errors, and increasing communication reliability have become new research objectives. The performance of vehicle platoon control depends on the

topology and quality of wireless communications. [5] investigated a constant time headway-based platoon control mechanism under limited communication range and random packet loss conditions. [6] studied the longitudinal control problem of vehicles based on a uniform constant time headway strategy, theoretically analyzing the upper bound of time delay to ensure platoon stability under packet loss conditions. To better address data transmission under constrained communication resources, [7] proposed a dynamic event-triggered mechanism to mitigate the impact of network topology on control performance in VANET. [8] designed a dynamic event-triggered mechanism for vehicles that considers unknown external disturbances and uncertain control inputs. This mechanism adaptively adjusts communication based on vehicle state variations and bandwidth availability, thereby improving communication performance. A platoon control framework was designed to maintain robust control performance even under random network topology variations. [9] examined the transmission mechanism of Cooperative Awareness Messages (CAMs) and developed a sampled-data feedback controller to eliminate the effects of random packet loss and external disturbances. For Vehicular Cyber-Physical Systems (VCPS), [10] considered the beamforming scheme on the control performance, and formulated the control optimization with the constraints of transmit power and beamwidth. By leveraging network topology information as a parameter, the control performance was further optimized. These studies comprehensively consider the impact of data communication on vehicle platoon control, demonstrating various approaches to enhance control performance under challenging communication conditions.

Current research has addressed these challenges through co-design approaches that jointly consider communication and control problems. [11] derived the transmission delay allowed to guarantee a required control performance. [12] and [13] found appropriate transmission scheduling schemes using the node mobility information which is provided by the node control function, while the works did not consider the impact of data transmission on control performance. [14] firstly found a transmission time slot allocation with the tracking control constraint, and then performed control optimization based on the specific allocation scheme. In other words, the work also considered the impact of communication on control performance. In [15], the maximum wireless system delay requirements are derived to guarantee the control system stability. Afterwards, the work designed the transmission scheme to meet the control system's delay needs. A very related work [16] proposed to use relays to extend the transmission range of platoon messages. The work firstly formulated an integer programming to derive the optimal relay selection with maximizing the link signal quality. Afterwards, a control optimization problem was constructed considering the uncertainty of packet receiving. In words, the routing problem and the control problem were not jointly optimized in [16]. Generally speaking, the existing works either study the impact of communication on control performance, either design the communication scheme to meet

the control system requirement.

III. PRELIMINARIES

A. Notations

We use uppercase letters to represent matrices and lowercase bold letters to represent vectors [17]. We denote the (i, j) entry of a matrix A with A_{ij} . We denote a graph $G = \{N, E\}$ consisting of n nodes $N = \{n_1, n_2, \dots, n_n\}$ and l edges $E \subseteq N \times N$, where $(n_i, n_j) \in E$ captures the existence of a link from node n_i to node n_j . A graph is connected if an undirected path exists between all pairs of nodes, where each edge (n_i, n_j) is associated with a non-negative weight $w_{ij} \geq 0$. The neighborhood \mathcal{N}_i of node n_i is defined as the set of adjacent nodes $n_j | (n_i, n_j) \in E$. The weighted Laplacian matrix L is then defined with off-diagonal entries $L_{ij} = -w_{ij}$ when $(n_i, n_j) \in E$, zero otherwise, while its diagonal entries satisfy $L_{ii} = \sum_{j \neq i} w_{ij}$ to ensure the zero-row-sum property.

B. Control Barrier Function

We consider the following control affine system:

$$\dot{x} = f(x) + g(x)u \quad (1)$$

where state $x \in \mathbb{R}^n$, input $u \in \mathbb{R}^m$, and Lipschitz continuous dynamics $f : \mathcal{D} \rightarrow \mathbb{R}^n$ and $g : \mathcal{D} \rightarrow \mathbb{R}^{n \times m}$.

Definition 3.1 [18] We define a set \mathcal{C} for the system (1). Let \mathcal{C} be forward invariant, if $x_0 \in \mathcal{C}$ implies that $x \in \mathcal{C}$ for all $k \in \mathcal{T}$. Therefore, we call the system (1) safe with the set \mathcal{C} .

Definition 3.2 [18] A set $\mathcal{C} \in \mathcal{D}$ is a 0-superlevel set of a continuously differentiable function $h : \mathcal{D} \rightarrow \mathbb{R}$ when

$$\mathcal{C} = \{x \in \mathcal{D} : h(x) \geq 0\} \quad (2a)$$

$$\partial\mathcal{C} = \{x \in \mathcal{D} : h(x) = 0\} \quad (2b)$$

$$\text{Int}\mathcal{C} = \{x \in \mathcal{D} : h(x) > 0\} \quad (2c)$$

Definition 3.3 [18] Let $\mathcal{C} = \{x \in \mathbb{R}^n | h(x) \geq 0\}$ express as the 0-superlevel set of a continuous function $h : \mathbb{R}^n \rightarrow \mathbb{R}$. The function h is a control barrier function (CBF) for (1) on \mathcal{C} if there exists an $\alpha \in [0, 1]$ for each $x \in \mathbb{R}^n$, there exists $u \in \mathbb{R}^m$ such that:

$$h(x) \geq \alpha h(x) \quad (3)$$

IV. SYSTEM MODEL

A. Vehicle Model

We consider a nonholonomic vehicle [18] described by

$$\dot{p}_x = v \cos \psi, \dot{p}_y = v \sin \psi, \dot{\psi} = u_1, \dot{v} = u_2 \quad (4)$$

where $p \triangleq [p_x, p_y]^T$ is the Cartesian coordinates of the vehicle, $v \triangleq \dot{p}$ is the linear velocity, $\psi \in (-\pi, \pi]$ is the orientation, and $v \in \mathbb{R}$ is the velocity. The turning rate $r \triangleq \dot{\psi}$ and acceleration $a \triangleq \dot{v}$ are controlled through the inputs $u \triangleq [u_1, u_2]^T \in U$. The space of admissible inputs is defined by

$$U = \{u \in \mathbb{R}^2 : |r| \leq r_{\max}, |a| \leq a_{\max}\} \quad (5)$$

where $r_{\max}, a_{\max} > 0$ represent the maximum rotation rate and acceleration, respectively. We denote that this system can be expressed in the control affine form (1) with $\mathbf{x} \triangleq [\mathbf{p}^T, \psi, v]^T \in \mathcal{D}$ and $\mathbf{g} = [0 \ \mathbf{I}]^T$ denote the zero and identity matrices, respectively.

B. Velocity Limitation

Rapid velocity fluctuations significantly impact the collision cone. Due to the constraints imposed by multiple driving modes, unpredictable velocity variations introduce substantial safety risks to the system. Therefore, accurately determining vehicle velocity is critical.

Each vehicle follows its designated trajectory at velocity v . The velocity cones enable to predict and determine collision-free motion constraints. The relative movement between vehicles is defined by velocity vector $\mathbf{v}_{j,i} \triangleq \mathbf{v}_i - \mathbf{v}_j$. If the velocity vector points toward the center of vehicle j within the distance $d_{\min,j}$, indicating that vehicle i will lead to a collision with vehicle j if both maintain their velocities with its current trajectory. This critical interaction zone is formally defined as the collision cone, expressed as:

$$\beta_{ij} \triangleq \arcsin \left(\frac{d_{\min,j}}{d_j} \right) \quad (6)$$

where $d_j \triangleq \|\mathbf{r}_j\|_2$, $\mathbf{r}_j \triangleq \mathbf{p}_j - \mathbf{p}$ represents the vector starting at the vehicle origin connecting to the center of vehicle j . Then the conditions that the velocity cone needs to meet as $\lambda_i < \beta_i$, the angle between $\mathbf{v}_{j,i}$ and \mathbf{r}_j is defined as

$$\lambda_{ij} \triangleq \arccos \left(\frac{\mathbf{v}_{j,i}^T \mathbf{r}_j}{\|\mathbf{v}_{j,i}\|_2 d_j} \right) \quad (7)$$

Lemma 1 [18]. Given that vehicle i will not collide with vehicle j at time $\tau \geq 0$ for all $\mathbf{v}_{j,i} \neq 0$ if

$$\lambda_{ij}(k) \geq \beta_i(k), \forall k \geq \tau \quad (8)$$

The velocity cone serves as a critical safety mechanism. However, there are heterogeneous vehicle types with complex behavioral patterns in complex traffic environments. The limitation of velocity is also decided by the driving operation of the proceeding vehicle f_i . To enhance the safety of vehicle, we consider the inter-vehicle distance $\Delta \mathbf{p}_{if_i} \triangleq \mathbf{p}_i - \mathbf{p}_{f_i}$. Let define the differential inter position [20] $\zeta_{if_i} = [\zeta_{px}, \zeta_{py}]^T = [p_{x_i} - p_{x_{f_i}}, p_{y_i} - p_{y_{f_i}}]^T$. We also define $D_{i[f_i]}(p_{x_i}, p_{x_{f_i}}) = \sqrt{(p_{x_i} - p_{x_{f_i}})^2 + (p_{y_i} - p_{y_{f_i}})^2}$. The operation of vehicle are divided into three typical behaviors: following, braking and changing lanes. Given the inter-vehicle distance Δp_{if_i} as the basis for the control barrier function formulation, the corresponding safety function h_{if_i} is defined as

$$h_{i,f_i}(p_i, p_{f_i}) = \begin{cases} D_1^2(p_i, p_{f_i}) - (2W)^2, & \text{if vehicle follows others} \\ D_2^2(p_i, p_{f_i}) - (2W)^2, & \text{if vehicle brakes in time} \\ D_3^2(p_i, p_{f_i}) - (2W)^2, & \text{if vehicle changes lanes} \end{cases} \quad (9)$$

where $W = \max\{W_1, W_2\}$ represents the safe radius of the safe collision zone, the value of W_1, W_2 are determined by the width of lanes. The predicted distance of avoiding collisions is $D_1 = \sqrt{(\Delta p_{if_i} - l_i^w)^2}$. The following mode depends solely on the Euclidean distance to the preceding vehicle f , l_i^w is the length of vehicle. $D_2 = \sqrt{(\Delta p_{if_i} - l_i^w)^2 + D^1}$, $D^1 = v_i(k)\tau_1 + \frac{v_i^2(k)}{2a_{\max}}\tau_1$ represents the response time introduced by the braking action of vehicle i . The safe distance of lane-changing is $D_3 = \sqrt{(\Delta p_{if_i} - l_i^w)^2 + D^2 + D^3}$, $D^2 = v_i(k)\tau_2 + \frac{1}{2}a_{\max}\tau_2^2$ and $D^3 = \frac{(v_i(k) + a_{\max}\tau_3)^2 - v_i(k)^2}{2a_{\max}}$. The separation distance D^1, D^2 and D^3 for each segment is computed based on the respective travel distances during different operational phases (including braking deceleration and accelerated lane changes), taking into account the characteristic response times at each stage of vehicle i . τ_2 and τ_3 are the response time of two stages in the mode of lane-changing.

Subsequently, we analyze the transmission model, taking into account the complex motion dynamics of vehicles within the system, to identify an optimal transmission path that enhances global system performance and ensures reliable velocity information exchange between vehicles.

C. Communication Model

In this paper, each vehicle can exchange control solutions and data with neighboring vehicles via V2V communication, while simultaneously transmitting service requests to roadside infrastructure through V2I links. The communication path loss between vehicle i and vehicle j [21] is intoline-of-sight (LoS) channel,

$$PL_{i,j}^{\text{LoS}} = 20 \log \left(\frac{4\pi f_c}{c} \right) + 20 \log(\Delta p_{ij}) + \eta_{\text{LoS}} \quad (10)$$

where η_{LoS} is parameters for the LoS channels. Δp_{ij} is the euclidean distance between the nodes, f_c is the carrier frequency and c is the speed of light. Analogously, the V2I path loss between vehicle i and roadside unit (RSU) I_j follows the same propagation model, with the separation distance Δp_{iI_j} defined as the 2D ground projection. The temporal variation in Δp_{iI_j} directly impacts the instantaneous channel conditions.

Then, we denote the signal-to-noise ratio (SINR) from two nodes as

$$\text{SINR}_{ij} = P^{TX} - PL_{ij}^{\text{LoS}} - N_{\text{noise}} \quad (11)$$

where P^{TX} is the power of transmitted signal and N_{noise} is the noise power (dB). Therefore, the transmission rate R of data between two nodes i and j according to the Shannon capacity formula is calculated by

$$R_{ij} = B_{ij} \log_2 \left(1 + 10^{\frac{\text{SINR}_{ij}}{10}} \right) \quad (12)$$

where B_{ij} denotes the bandwidth of the communication channel of link l_{ij} .

We establish a minimum SINR threshold ξ_0 for successful vehicular data reception. The transmission is considered successful when the aggregate SINR at receiver i satisfies $\xi_i \geq \xi_0$,

ξ_i denotes the amount of data received by vehicle i in this communication link. Thus, the state model can be obtained as follows [18]:

$$x_i(k+1) = \mathbf{A}x_i(k) + \mathbf{F}u_i(k) + \delta_{ij}(k) \cdot (x_j(k) - x_i(k)) \quad (13)$$

where \mathbf{A} and \mathbf{F} are matrices describing the entire system. The probability of δ_{ij} is calculated by the probability of successfully receiving data $P = Pr(\xi_{ij} \geq \xi_0)$. If vehicle i successfully receives data of vehicle j at the time slot k , let $\delta_{ij}(k) = 1$, otherwise, $\delta_{ij}(k) = 0$. $Pr(\delta_{ij} = 1) = Pr(\xi_{ij} \geq \xi_0)$, $Pr(\delta_{ij} = 0) = 1 - Pr(\delta_{ij} = 1)$.

V. JOINT OPTIMIZATION SCHEME

We propose to design a joint optimization mechanism that optimizes vehicle trajectories while ensuring traffic performance based on control theory, simultaneously incorporate node mobility awareness in routing to enhance transmission stability. This integrated approach will further improve data reliability and consequently refine control performance. The detailed design methodology is presented in the following sections.

A. The Optimal Path of Transmission

The transmission path performance is jointly determined by both the inter-node link quality and the individual node characteristics [22]. To comprehensively evaluate the current path's transmission capability, we establish a metric system encompassing node-level and link-level performance indicators.

1) Node characteristics of transmission:

- **Vehicle status.** The status of vehicle i represents its capability to process the current transfer request. The status is formally defined as vs_i , let $vs_i = 1$, if $q_i \leq q_{max}$. $vs_i = 0$, otherwise. q_i indicates the length of the current processing queue of vehicle i , and q_{max} indicates the upper limit of the maximum processing queue.
- **Number of neighbor vehicles.** Let \mathcal{N}_i^{path} denote the number of neighboring vehicles for vehicle i in this transmission path, while the current transmission performance of vehicle i is evaluated as $\mathcal{N}_i^{path} = \sum_{i=1}^n vs_i$.
- **Relay reliability.** The relaying reliability R_r of the i_{th} vehicle quantifies its transmission reliability when performing relaying tasks. Mathematically, it is defined as the ratio between successfully relayed tasks and the total number of tasks received for relaying, expressed as $R_r = \frac{\text{Number of task relayed}}{\text{Total number of task received for relay}}$.

2) *Link-level characteristics of transmission:* This paper designs a new link metric that fully considers the mobility of vehicles, particularly the impact of their velocity, position, and direction on transmission path vulnerability, disruption, and overhead. The specific link metric is as follows.

Staying time. Vehicles can only communicate when they are within each other's transmission range. The residence time is defined as the duration for which vehicle i remains within

the communication range of vehicle j . Based on their velocity v_i and v_j , the duration time of link is denoted as:

$$sd_j^i = \frac{R_v - \Delta p_{ij}}{|v_i - v_j|} \quad (14)$$

where, R_v is communication range of vehicles and Δp_{ij} is distance between two vehicles.

Direction ratio. We preferentially select neighbor vehicles with matching movement directions as relay nodes. The direction ratio is given as:

$$d_{\Delta p_{ij}} = \frac{\Delta p_j^z}{\Delta p_s^z} \quad (15)$$

where Δp_j^z denotes the vector between vehicle j and the destination node z based on the difference of spacing distance, while Δp_s^z denotes the vector between the source node s and the destination node z .

Velocity variance. To maintain stable transmission paths with highly dynamic nodes, we therefore define velocity variance σ_v to quantify the degree of variability or dispersion in motion direction and trajectory of vehicles.

$$\sigma_v = \sqrt{\frac{\sum_{j=1, i \in N}^z (v_i - \bar{v})^2}{z}} \quad \bar{v} = \frac{\sum_{j=1, i \in N}^z v_i}{z} \quad (16)$$

where \bar{v} is the mean of the velocity of vehicles in the path. Vehicle i can only obtain current velocity of vehicle j at time slot k if the transmission succeeds; otherwise, it must rely on the historical velocity of vehicle j .

Distance variance. In wireless network scenarios, as the number of vehicles grows and transmission demands increase within the network system, transmissions from neighboring nodes can cause interference to the current node. We define the probability of successful transmission of V2I or V2V links is expressed as $P_{ij}(\theta_{ij})$, packets are transmitted within multiple time slots, $\theta_i(k)$ represents the amount of data (bits) transmitted by vehicle j to vehicle i in time slot k .

$$\begin{aligned} & prob_{ij}(\theta_i(k), v_i(k), v_j(k)) = \\ & \exp \left(- \frac{2^{\frac{\theta_i(k)N}{B\tau_l}} - 1}{\varpi_{ij}} \cdot L_{ij}^2(v_i(k), v_i(k), v_j(k), \dot{v}_j(k)) \right) \end{aligned} \quad (17)$$

The time-varying relative distance L_{ij} [6] between the node j and node i , $L_{ij}(v(k), \dot{v}(k)) = \sqrt{[p_j(k) - p_i(k)]^2 + L_0^2}$, L_0 is represented the relative vertical distance between vehicles and infrastructures. L_{ij} is related to the control vector and system model. N is the number of vehicles contending the same channel simultaneously. B is the bandwidth of this channel and τ_l is the length of time slot, where ϖ_{ij} represents the normalized power parameters related to SINR. Similarly, the current velocity $v_j(k)$ can only be obtained if the data transmission is successful.

If the data is transmitted in multiple time slots (total data volume), the total successful probability of this link is followed as:

$$P_{ij}(\theta_i(k), v_i(k), v_j(k)) = \prod_{k=1}^K \text{prob}_{ij}(\theta_i(k), v_i(k), v_j(k)) \quad (18)$$

Path value. Based on these metrics, we utilize the path metric as an optimization criterion to identify the optimal transmission path. We optimize the transmission path by selecting transmitting nodes based on path value, which evaluates the impact of each candidate node in $\mathcal{N}_i^{\text{path}}$. The optimal path is constructed step by step using the highest value at each node. The value is calculated as follows:

$$\Delta_{\text{path}} = \frac{sd_j^i \times w_i \times d_{\Delta p_{ij}}}{\sigma_v} \times P_{ij}(\theta_i(k), v_i(k), v_j(k)) \quad (19)$$

where w is the weight of node i is set by node characteristic. The weight of node i is calculated as:

$$w_i = \begin{cases} \kappa_1 \cdot v s_i + \kappa_2 \cdot \mathcal{N}_i^{\text{path}} \\ + \kappa_3 \cdot R_r^i, & \text{the node is able to transmit,} \\ 1, & \text{otherwise.} \end{cases} \quad (20)$$

where κ_1, κ_2 and κ_3 respectively represent the weight values corresponding to the features of each node.

B. The Control Scheme

Channel interference, link congestion, timeout and so on will cause communication problems, resulting in packet loss, in this paper we use the Markov packet loss model framework to accurately capture the stochastic nature of the packet loss process [21]. However, due to the problem of data packet loss existing in the communication transmission process, the vehicle need to ensure the safety of vehicle formation control and the stability of vehicle formation regardless of whether it can successfully receive the data packet at present. Based on this, we construct and design the following the control objective. We denote T to be the predictive horizon length. Let $K = \{0, 1, 2, \dots, T\}$. We define the cost function J as determined by the control input u , the deviation from the ideal trajectory \dot{x} , and the state x deviation among neighboring vehicles [23]. The cost function of vehicle i is defined as

$$J_i = \|u_i(k)\|_{R_i} + \|\dot{x}_i(k) - x_i(k)\|_{F_i} + \sum_{j \in N} \|\dot{x}_i(k) - x_j(k) - \Delta p_{ij}\|_{G_i} \quad (21)$$

where R and F are the positive definite matrix, G is the symmetric matrix. $x_i(k)$ represents the state of the control input predicted by vehicle i at time slot k . The predicted trajectory is denoted by $\dot{x}_i(k)$ with the predicted control input $u_i(k)$ and the initial state $x_i(k)$, where $x_i(0) = x_i(k)$.

However, vehicle i cannot maintain seamless communication with all neighboring vehicles at all times. During the time interval $[K-1, K]$, vehicle i continuously receives data until the transmission is fully completed. At this stage, vehicle i

cannot acquire the most recent data and must rely solely on historical data from the time interval $[0, K-1]$. To further mitigate the impact of unreliable data transmission on control performance, we define the self-deviation constraint as [23]:

$$\begin{aligned} & \gamma_i \sum_{k=1}^{T_p-1} \|\dot{x}_i(k) - x_i(k)\|_{G_i} \\ & \leq \sum_{k=1}^{T-1} \|\dot{x}_i(k-1) - x_i(k-1)\|_{G_i} \end{aligned} \quad (22)$$

Then the optimization problem [23] is designed as:

$$\min_{u_i(k), k \in \mathbb{K}_0} J_i = \sum_0^{K-1} J_i(k) + \delta_{ij}(k) \sum_{K-1}^K J_i(k) \quad (23a)$$

$$\text{s.t.} \begin{cases} x_i(k+1) = A x_i(k) + F u_i(k) \\ + \delta_{ij}(k) \cdot (x_j(k) - x_i(k)), \\ \gamma_i \sum_{k=1}^{T-1} \|\dot{x}_i(k) - x_i(k)\| \\ \leq \sum_{k=1}^{T-1} \|\dot{x}_i(k-1) - x_i(k-1)\|, \\ a_{\min} \leq \bar{v} \leq a_{\max}, v_{\min} \leq v \leq v_{\max} \\ \psi_{\min} \leq \psi \leq \psi_{\max}, r_{\min} \leq r \leq r_{\max} \\ h_{i,j}(p_i, p_j) \geq -\alpha(h_{i,j}), \forall i, j \in N \\ \lambda_{ij}(k) \geq \beta_{ij}(k), \forall k \geq \tau, \forall i, j \in N \end{cases} \quad (23b)$$

where γ_i is a scale coefficient. These constraints are initial state, control input constraints, the vehicle dynamics constraints, CBF constraints and self-deviation constraint to ensure system stability under random packet loss.

C. The Transmission Optimization Scheme

The data packet transmission optimization can be formulated as an integer programming problem over the time horizon T_p . The optimization [24] involves two key decision variables the packet scheduling Z_ℓ^{mk} and routing decisions y_l^{gk} , where $y_l^{gk} \in \{0, 1\}$ indicates whether the arriving packet is scheduled using relative path l at time k , l represents the communication link of node i and node j . The channel activation variables which represent the network scheduling decisions.

$$\max \sum_{k=0}^K \sum_{g=1}^{\Theta_k} \sum_{\ell \in L} y_l^{gk} \Delta_{\text{path}} \quad (24a)$$

$$\text{s.t.} \begin{cases} \sum_{\ell \in L} y_l^{gk} \leq 1, \\ \sum_{\tau=k-k_{\max}}^{\tau \wedge K} \sum_{g=1}^{\Theta_k} \sum_{l: l_{k-\tau}=\ell} y_l^{g\tau} \leq \sum_{m=1}^M \sum_{l: \ell \in l} Z_\ell^{mk}, \\ \sum_{\ell \in L} Z_\ell^{mk} \leq 1, \quad \forall m \in [M], k \in [K], \ell \in [L] \\ Z_\ell^{mk} \in \{0, 1\}, \quad \forall m \in [M], k \in [K], \ell \in [L] \\ y_l^{gk} \in \{0, 1\}, \quad \forall k \in [K], l \in [L]. \end{cases} \quad (24b)$$

where Z_l^{mk} indicates that at each time and channel, one independent set is selected for the network schedule. Θ_i is denoted to be the sum of data of the transmission target from node i . m and g represent the number of channel and the number of packets respectively. The term $(k - k_{max})$ denotes the remaining time slots from the arrival slot k until the deadline for a packet. This constraint guarantees that for any time slot and arriving packet, the total scheduled transmissions of packet on link l during the interval $[k, k + k_j]$ cannot exceed the number of channels allocated to link l .

D. The Joint Optimization

To achieve optimal data transmission in vehicular networks, the platoon must account for both the complexity of vehicle dynamics and the challenges posed by unreliable communication channels. More precise vehicle trajectory prediction enables the system to select optimal transmission paths, while transmission optimization significantly reduces packet loss probability. Consequently, we formulate a dual-objective optimization DynaRoute framework that simultaneously: (1) maximizes transmission performance and (2) minimizes formation oscillation. Building upon this foundation, we propose a joint optimization model for vehicular communication networks. This comprehensive model integrates key aspects of vehicle mobility, formation control theory, and communication reliability, formally expressed as follows:

$$\begin{aligned} & \max_{u,v,p} Y(u,v,p) \\ & \min_u J(u) \\ \text{s.t.} \quad & \begin{cases} x_i(k+1) = Ax_i(k) + Fu_i(k) \\ \quad + \delta_{ij}(k) \cdot (x_j(k) - x_i(k)), \\ h_{i,j}(p_i, p_j) \geq -\alpha(h_{i,j}), \forall i, j \in N \\ \lambda_{ij}(k) \geq \beta_{ij}(k), \forall k \geq \tau, \forall i, j \in N; \\ u_i(k) \geq 0, \quad i \in N, k \in K \\ \delta_{ij}(k) \in \{0, 1\}. \end{cases} \end{aligned} \quad (25)$$

We convert the minimization problem $\min_u : J(u)$ to the minimization problem $\max_u : -J(u)$. Next, we calculate the maximum optimization objective of the new optimization $Y(u,v,p) - J(u)$. The optimization problem is solved by Nondominated Sorting Genetic Algorithm(NSGA) [25].

E. Iterative Optimization Algorithm

This paper proposes a collaborative transmission optimization mechanism based on the improved NSGA-II algorithm and DMPC controller algorithm [23]. While ensuring reliable platoon control performance, optimization is conducted in the communication link selection with desire position p^* , velocity v^* and acceleration a^* . The solution of (23) guides vehicles for optimal control performance. We transform the optimization problems into maximization problem. The process is as follows.

According to the aforementioned algorithm, the optimal solution is obtained as $u^* = \arg \min_{u \in \mathcal{U}} J(u)$. The solution of (25) for a set of path values under the current node's motion

Algorithm 1 Distributed Model Predictive Control for Vehicle Platooning

Input:

- Initialization state x_0
- Maximum calculation times $CalMax$
- Vehicle constraints of u, v, p

Output: Pareto-optimal solutions u^*

Initialization of the leader vehicle $k = 0$: for $i \in N$ do

a) Prearrange $x_i(0)$ and $u_i(0)$:

$$x_i(0) = \begin{cases} x_i(0), & k = 0, \\ Ax_i(k-1) + Fu_i(k-1), & k \in K. \end{cases}$$

$$u_i(0) \in U_i, \quad k \in K.$$

Online Phase at following vehicle $k \geq 0$: for $i \in N$ do

- Convey $x_i(k)$ to vehicles $j \in N$;
- Receive $x_j(k)$ from vehicles $j \in N$;
- Resolve the probability using Markov states, then attain $u_i^*(k)$ and $x_i^*(k)$;
- Resolve the probability of δ_{ij} , determine whether neighbor states are successfully acquired;
- Take $u_i^*(0)$ for the control of vehicle i ;
- Prearrange $x_i^*(k+1)$ and $u_i^*(k+1)$:

$$x_i^*(k+1) = \begin{cases} x_i^*(k), & \text{if vehicle failed,} \\ Ax_i(k) + Fu_i(k) + \delta_{ij}(k) \cdot (x_j(k) - x_i(k)), & \\ \text{if vehicle succeeded.} \end{cases}$$

$$u_i^*(k+1) = \begin{cases} u_i^*(k), & \text{if vehicle failed,} \\ \sum_{j \in N} \delta_{ij}(k) (x_j(k) - x_i(k) - \Delta p_{j,i}), & \\ \text{if vehicle succeeded.} \end{cases}$$

Iteration at $t \geq 0$: for $i \in N$,

- Set initial solution and candidates:

solution _{i} (0) $\leftarrow \emptyset$, candidates _{i} (0) $\leftarrow \text{getInitialCandidates}()$

- Select candidate with maximum value:

$$u_i^*(t) \leftarrow \arg \max_{c \in \text{candidates}_i(t)} J(c)$$

- Update solution if feasible:

$$\text{solution}_i(t+1) \leftarrow \begin{cases} \text{solution}_i(t) \cup \{u_i^*(t)\} \\ \text{if isFeasible}(u_i^*(t)), \\ \text{solution}_i(t), \text{otherwise.} \end{cases}$$

- Prune candidates:

$$\text{candidates}_i(t+1) \leftarrow \begin{cases} \text{candidates}_i(t) \setminus \{u_i^*(t)\} \\ \text{if isFeasible}(u_i^*(t)), \\ \text{candidates}_i(t), \text{otherwise.} \end{cases}$$

- Check termination:

If isTerminal(solution _{i} ($t+1$)), return solution _{i} ($t+1$).

based on p^* , v^* and a^* , determining the selection for each hop. Therefore, at the timestep k , for the current node i , the next-hop node j and transmission channel g are selected based on the value of optimization in (25) derived from a set of hop-by-hop determined y_l^{gk} . Through multiple iterations, we optimize and determine the desired solution and select the maximum value as the optimal solution by calculating the value of optimization in (25).

To address the two joint optimization objectives, the NSGA-II algorithm is employed to solve the joint multi-objective optimization problem. The detailed algorithm is as follows:

Step 1: We first define an empty set $\mathcal{Y}_0 = \{y_l^{gk} = 0 | k \in K, l \in L, g \in \{0, 1, 2, \dots, \Theta\}\}$ to store the resulting candidate solutions y_l^{gk} , where $l \in [L]$ at initial iteration 0. We acquire the current network topology in VANET, we first construct a link set derived from the neighborhood relationships between the source and destination nodes. By traversing the entire dynamic topology, we generate a collection of transmission decision schemes. And then we store the set of solutions in collection $\mathcal{Y}_0 = \{y_l^{gk}(0) = 0 | k \in K, l \in L, g \in \{0, 1, 2, \dots, \Theta\}\}$, thereby obtaining the initialized set $\mathcal{Y}_t = \{y_l^{gk}(t) | k \in K, l \in L, g \in \{0, 1, 2, \dots, \Theta\}\}$ at iteration t .

Step 2: We employ a set of predefined reference points to ensure diversity in the obtained solutions. Based on three indicators as u, v, p , each indicator is partitioned into 10 segments according to reference location coordinates, adaptively generating 55 reference points [27]. The algorithm for selecting reference points is as follows:

Let C be a two-dimensional variable defined over the domain $0, \frac{1}{10}, \frac{2}{10}, \dots, \frac{11}{10}$, where c_{ij} represents the evenly distributed parts of the three indexes of u, v, p . For each $c_{ij} \in C$, $c_{ij} = c_{ij} - \frac{j-1}{10}$. We rank the individuals within $\mathcal{Y}_t = \{y_l^{gk}(t) | k \in K, l \in L, g \in \{0, 1, 2, \dots, \Theta\}\}$ based on reference points to effectively enhance solution diversity.

Step 3: We perform non-dominated sorting on $\mathcal{Y}_t = \{y_l^{gk}(t) | k \in K, l \in L, g \in \{0, 1, 2, \dots, \Theta\}\}$. Based on the calculations of two optimization functions in (25), the corresponding values are obtained and assigned. Then the set $\mathcal{Y}_t = \{y_l^{gk}(t) | k \in K, l \in L, g \in \{0, 1, 2, \dots, \Theta\}\}$ undergoes non-dominated sorting and crowding distance calculation to select parents, followed by crossover and mutation operations to generate suitable offspring. Then we construct the new set $\mathcal{Y}' = \{y_l^{gk}(t) | k \in K, l \in L, g \in \{0, 1, 2, \dots, \Theta\}\}$. The basic steps are as follows:

We select individuals $y_{l_1}^{gk}(t)$ and $y_{l_2}^{gk}(t)$ from $\mathcal{Y}_t = \{y_l^{gk}(t) | k \in K, l \in L, g \in \{0, 1, 2, \dots, \Theta\}\}$ after sorted with lower non-dominated ranks and higher dynamic crowding distances through tournament selection, then generate offspring $y_{l_1}^{gk}(t+1)$ and $y_{l_2}^{gk}(t+1)$ of the iteration t to proceed to compute and update.

Step 4: According to the above mutation calculations, we

obtain the new values of offspring are obtained and stored in the set \mathcal{Y}' and we construct the set $\mathcal{Y}_{t+1} = \mathcal{Y}_t \cup \mathcal{Y}'$, where $\mathcal{Y}_{t+1} = \{y_l^{gk}(t+1) | k \in K, l \in L, g \in \{0, 1, 2, \dots, \Theta\}\}$. The values retained from the previous two steps and the newly calculated values are then merged to form the set \mathcal{Y}_{t+1} for the next iteration $t+1$.

Step 5: For the iteration $t+1$, we first judge whether the algorithm has met the termination condition. If $t+1$ exceeds the maximum iteration count $GenMax$, terminate the algorithm and output the non-dominated solutions in $\mathcal{Y}_t = \{y_l^{gk}(t) | k \in K, l \in L, g \in \{0, 1, 2, \dots, \Theta\}\}$ as the Pareto optimal set, the optimal transmission path is determined based on the corresponding optimal values following the calculation of the value of optimization in (25) and then we select the maximum value. The transmission path scheme corresponding to the maximum value is then identified as the optimal solution, we then get the best value of the set y_l^{gk} ; otherwise, continue executing the NSGA-II algorithm from the above steps until we choose the optimal transmission. The algorithm is shown as follows.

VI. PERFORMANCE EVALUATION

This section presents a comprehensive evaluation of the proposed dual-objective joint optimization model through systematic simulation studies. First, we provide a detailed description of the simulation environment and parameter configurations. Subsequently, we present an in-depth analysis of the optimization model's performance metrics. Finally, to rigorously validate the proposed approach, we conduct comparative experiments assessing both V2I communication reliability and platoon control stability. All numerical simulations were executed using python. The hardware configuration features an Xeon W-2135 processor (3.7 GHz base frequency, 64-bit architecture) with 32GB RAM, ensuring robust computational capability for the simulation scenarios.

A. Simulation Setup

The simulation environment comprises two parallel straight lanes populated with multiple Connected and Autonomous Vehicle (CAVs). In this setup, we deploy two distinct platoons, each consisting of four vehicles (one leader and three followers) operating on separate lanes, totaling eight CAVs in the simulation. We establish the vehicle mobility parameters are configured following the methodology in [2], while the V2I communication parameters are implemented according to [3]. For precise initialization, Table 1 comprehensively documents the complete parameter set governing fleet mobility dynamics and physical layer communication characteristics.

The scenario evaluates the resilience of connected vehicle systems. The simulation employs a 0.1s sampling interval for platoon control. We predefine the leading vehicle's acceleration and deceleration profiles, with detailed velocity

Algorithm 2 NSGA-II for Multi-Objective Optimization

Input:

- Population size N
- Maximum generations $GenMax$
- The maximum solution of $J(u^*)$

Output: Pareto-optimal solutions y^*

for $t \leftarrow 1$ to $GenMax$ **do**

Initialization at $t = 0$:

 a) Generate initial population:

$$\mathcal{Y}_t(i) \leftarrow \text{randomIndividual}(), \quad \mathcal{Y}'_t \leftarrow \emptyset$$

 b) Evaluate the first objective and constraints:

$$\max_{u,v,p} -J(u), \quad \forall u \in U$$

 c) Evaluate the second objective and constraints:

$$\max_{u,v,p} Y(y_l^{gk}), \quad \forall k \in K, l \in L, g \in \{0, 1, 2, \dots, \Theta\}$$

Generational loop at $t \geq 0$:

 a) Combine populations:

$$\mathcal{Y}_t \leftarrow \mathcal{Y}_t \cup \mathcal{Y}'_t$$

 b) Non-dominated sorting:

$$(y_{l_1}^{gk}, y_{l_2}^{gk}, \dots) \leftarrow \text{sortNonDominated}(\mathcal{Y}_t)$$

 c) Crowding distance calculation with the first objective:

- $\text{Distance}(x) \leftarrow \sum_{k=1}^m \frac{Y(y_{l_i}^{gk}) - Y(y_{l_{i+1}}^{gk})}{Y^{\max} - Y^{\min}}$
- $\forall k, l, g$

 d) Crowding distance calculation with joint objective:

- $\text{DISTANCE}(x) \leftarrow \sum_{k=1}^m \frac{-J(u_i) + J(u_{i+1})}{(-J^{\max}) - (-J^{\min})}$
- $\forall u \in U$

 e) Crowding distance calculation with the second objective:

$$\text{distance}(x) \leftarrow \text{Distance}(x) - \text{DISTANCE}(x),$$

 f) Population selection:

$$\mathcal{Y}_{t+1} \leftarrow \bigcup_{i=1}^l y_{l_i}^{gk} \quad \text{until } |\mathcal{Y}_{t+1}| + |\mathcal{Y}'_{t+1}| > N$$

 g) Generate offspring:

$$\mathcal{Y}'_{t+1} \leftarrow \text{tournamentSelect}(\mathcal{Y}_{t+1}) \oplus \text{adaptive crossover/mutation}$$

 h) Termination:

$$\text{If } t + 1 = GenMax, \text{ return } \text{ParetoFront}(\mathcal{Y}_t).$$

end for

TABLE I
PARAMETERS SETTINGS IN MODEL

Parameter	Value	Parameter	Value
ϵ	3×10^{-5}	d_i	10 m
a_{\min}	-2.5 m/s^2	a_{\max}	$+2.5 \text{ m/s}^2$
ξ_{\min}^v	-6 m/s	ξ_{\max}^v	$+6 \text{ m/s}$
ξ_{\min}^p	-3 m	ξ_{\max}^p	$+3 \text{ m}$
Θ_i	$5 \times 10^9 \text{ bits}$	B	10 Mbit
ϖ	-96 dBm	K	30 s
L_0	50 m	$L_{V2I,0}$	200 m

variation patterns. The accelerations and decelerations of the lead vehicle is shown as:

$$a_0(k) = \begin{cases} 0.5 \text{ m/s}^2, & k \in [3.5, 5.5] \text{ s} \\ 1 \text{ m/s}^2, & k \in [6.0, 7.5] \text{ s} \\ 0.5 \text{ m/s}^2, & k \in [8.0, 10.0] \text{ s} \\ -0.5 \text{ m/s}^2, & k \in [14.5, 16.5] \text{ s} \\ -1 \text{ m/s}^2, & k \in [17.0, 18.5] \text{ s} \\ -1 \text{ m/s}^2, & k \in [19.0, 21.0] \text{ s} \\ 0 \text{ m/s}^2, & \text{others} \end{cases} \quad (26)$$

B. Experimental Results

Experiment 1 examined the transmission performance of two mechanisms in VANET. The first method is the joint optimization method designed in this paper. The second method is the Artificial Intelligence-aware Emergency Routing Protocol. This method constructs a Belief-Desire-Intention (BDI) model to understand the environment, integrating data such as traffic density, congestion levels, collision signals, and hazard detection to optimize route selection for the system. We have respectively implemented the intelligent transportation system routing protocols based on decentralized Model Predictive Control (DMPC) [21] and artificial intelligence (AI) [26] of Emergency routing protocol (ERP) in the vehicle queue as reference comparisons.

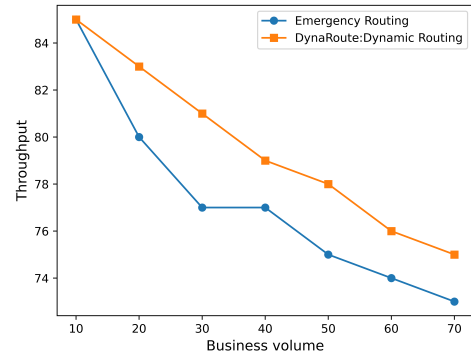


Fig. 1. Throughput under different network load levels

As shown in Fig. 1-4, the horizontal axes represent network load and packet transmission interval, while the vertical axes include throughput and end-to-end delay. These figures illustrate the transmission performance curves of the vehicular

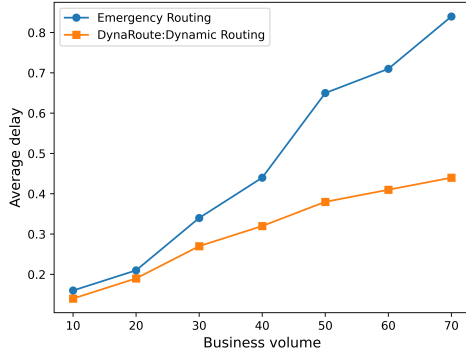


Fig. 2. End to end delay under different network load levels

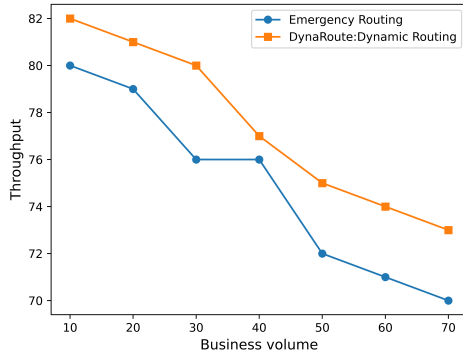


Fig. 3. Throughput under different packet interval levels

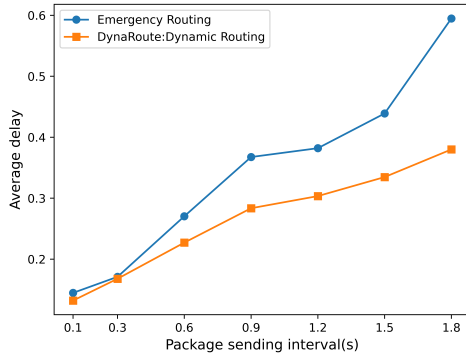


Fig. 4. End to end delay under different packet interval levels

network under different network loads and different packet interval levels. In Fig. 1, when the load is light, two mechanisms maintain satisfactory transmission performance. As the network load increases with the number of packets, the rising transmission delay raises end to end delay, leading to a significant performance degradation in ERP. As depicted in Fig. 3, as the number of data packets transmitted in the network increases, node load becomes heavier and transmission performance gradually deteriorates. The ERP fails to adequately account for dynamic link metrics, resulting in significant performance degradation. The joint optimization mechanism dynamically adjust link metrics, identifying optimal links that meet multiple criteria under varying network loads. Fig. 2 and Fig. 4 compare the packet transmission delays of the two mechanisms under different packet interval, ERP does not fully account for node mobility, leading to increased link fragility in complex vehicle movement scenarios, which slightly degrades its performance. As the load grows, this contention increases packet loss rates and substantially raises end-to-end delay. In contrast, the proposed mechanism consistently prioritize the most stable paths for vehicles, maintaining superior transmission performance despite load fluctuations caused by traffic variations. The results demonstrate that the proposed mechanism achieves stable transmission performance under varying network load conditions, exhibiting strong robustness against both node mobility and dynamic network loads.

Experiment 2 examined the impact of the joint mechanism on the dynamics of platoon formation. Under the condition of leading vehicle dynamics changes, the study analyzed the guidance of the joint optimization mechanism in this paper, taking into account the influence of communication interference between vehicles on the reception of control information such as velocity of neighbour vehicles. We investigated the time-varying patterns of the trajectories, vehicle distances, vehicle velocities and control inputs (acceleration) of eight vehicles within two platoons.

The two sets of figures illustrate that in both packet-loss scenarios for vehicular networks, vehicles require control mechanisms to compensate for errors and interference caused by transmission failures. Fig. 5-7 demonstrate the control performance under network packet loss conditions (case1), while Fig. 9-11 show the control performance in overloaded vehicular network systems with dense vehicle presence and severe packet transmission obstacles (case2). Fig. 5-11 present the real-time position, velocity, and acceleration of eight vehicles in two platoons under the joint optimization scheme proposed in this paper. As seen in Fig. 5 and Fig. 9, the inter-vehicle distance consistently remains greater than zero, effectively eliminating collision risks. Regardless of irregular velocity variations in the leading vehicle, all following vehicles maintain a safe following distance quickly through an appropriate response mechanism. The results in Fig. 6 and Fig. 10 reveal that in both platoons, vehicles 0-7 exhibit rapid velocity responses to changes in preceding vehicles. According to the definition of string stability in [29], both platoons maintain stability under these dynamic conditions.

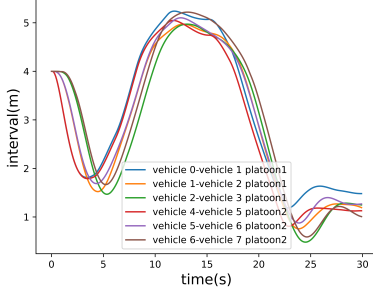


Fig. 5. interval distance in case1

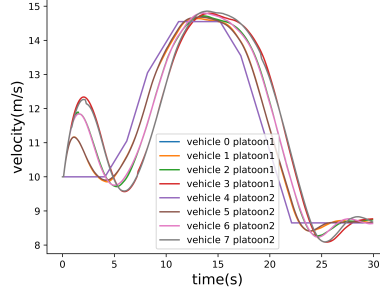


Fig. 6. velocity in case1

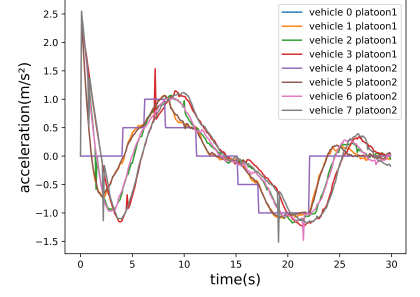


Fig. 7. acceleration in case1

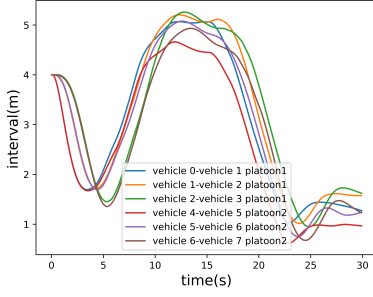


Fig. 8. interval distance in case2

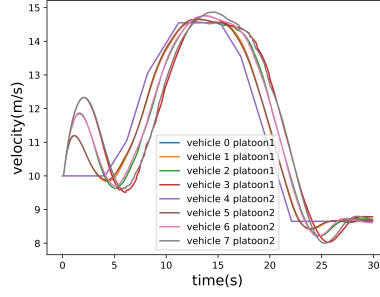


Fig. 9. velocity in case2

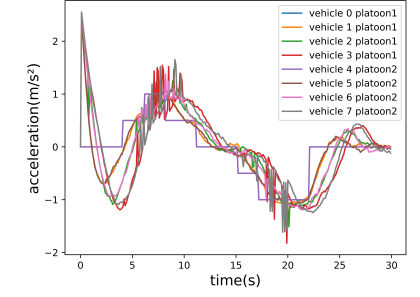


Fig. 10. acceleration in case2

Since vehicle acceleration is determined by control inputs, it proves most sensitive to variations. The acceleration curves in Fig. 7 show significant correlation with velocity values of adjacent vehicles, with all disturbance fluctuations strictly bounded within $\pm 1m/s^2$. The joint control mechanism effectively mitigates interference from packet loss and other transmission errors while consistently maintaining efficient platoon control performance. In Fig. 11, despite severe packet loss and fluctuating transmission performance, acceleration variations intense yet the fluctuations of disturbance are also bounded with $\pm 2m/s^2$. The control input always preserve safe driving. These empirical parameter variations demonstrate that the proposed mechanism can reliably guide vehicles to operate safely and efficiently in vehicular networks, even under potential information loss or transmission delays.

VII. CONCLUSION

We introduce DynaRoute, a new transmission optimization mechanism that leverages control mechanisms and precise node mobility prediction in Internet of Vehicles scenarios to simultaneously ensure safe vehicle guidance and maintain stable, reliable communication links for high-velocity mobility. DynaRoute enhances network throughput while minimizing link disruptions and handoffs caused by node movement. The mechanism employs computing to jointly solve control and transmission optimization problems, determining optimal solutions for multi-objective challenges and identifying ideal transmission paths for source-destination pairs. Our simulation-based evaluation demonstrates that the performance

of DynaRoute, whether measured by throughput, end to end delay, or driving safety metrics remains robust against common wireless network impairments including interference, channel contention, and packet loss.

REFERENCES

- [1] Y. Li and W. Chen and S. Peeta and Y.Wang, "Platoon control of connected multivehicle systems under V2X communications: Design and experiments," *IEEE Transactions on Intelligent Transportation Systems*, vol. 21, no. 5, pp. 1891–1902, 2020.
- [2] A. Martínez and E. cañibano and J. Romo, "Analysis of low cost communication technologies for V2I applications," *Applied Science*, vol. 10, no. 4, pp. 1249, 2020.
- [3] Q. Chen, Y. Zhou, S. Ahn, J. Xia, and S. Li, "Robustly string stable longitudinal control for vehicle platoons under communication failures: A generalized extended state observer-based control approach," *IEEE Transactions on Intelligent Transportation Systems*, vol. 8, no. 1, pp. 159–171, 2023.
- [4] V. Fooladi and P. Azmi and N. Mokari and H. Saeedi, "Innovative Segmentation-Based Routing in VANETs: Leveraging the Advantages of TD-ISAC," *TechRxiv*, 2025. [Online]. Available: <https://www.techrxiv.org/users/883240/articles/1262533-innovative-segmentation-based-routing-in-vanets-leveraging-the-advantages-of-tt-isac>.
- [5] C. Zhao and L. Cai and P. Cheng, "Stability Analysis of Vehicle Platooning With Limited Communication Range and Random Packet Losses," *IEEE Internet of Things Journal*, vol. 8, no. 1, pp. 262–277, 2021.
- [6] C. Zhao and X. Duan, L. Cai and P. Cheng, "Vehicle Platooning With Non-Idempotent Networks," *IEEE Transactions on Vehicular Technology*, vol. 70, no. 1, pp. 18–32, 2021.
- [7] S. Xiao and X. Ge and Q.-L. Han and Y. Zhang, "Dynamic event-triggered platooning control of automated vehicles under random communication topologies and various spacing policies," *IEEE Transactions on Cybernetics*, vol. 52, no. 11, pp. 11477–11490, 2022.

- [8] X. Ge and S. Xiao and Q.-L. Han and X.-M. Zhang and D. Ding, "Dynamic event triggered scheduling and platooning control co-design for automated vehicles over vehicular ad-hoc networks," *IEEE/CAA Journal of Automatica Sinica*, vol. 9, no. 1, pp. 31–46, 2022.
- [9] S. Wen and G. Guo, "Communication topology assignment and control co-design for vehicle platoons in LTE-V2V network," *IEEE Transactions on Vehicular Technology*, vol. 70, no. 12, pp. 12462–12476, 2021.
- [10] H. Zhu and Y. Zhou and X. Luo and H. Zhou, "Joint Control of Power, Beamwidth, and Spacing for Platoon-Based Vehicular Cyber-Physical Systems," *IEEE Transactions on Vehicular Technology*, vol. 71, no. 8, pp. 8615–8629, 2022.
- [11] X. Duan and Y. Zhao and D. Tian and J. Zhou, L. Ma and L. Zhang, "Joint Communication and Control Optimization of a UAV-Assisted Multi-Vehicle Platooning System in Uncertain Communication Environment," *IEEE Transactions on Vehicular Technology*, vol. 73, no. 3, pp. 3177–3190, 2023.
- [12] P. Zhang and D. Tian and J. Zhou and X. Duan and Z. Sheng and D. Zhao, "Joint Optimization of Platoon Control and Resource Scheduling in Cooperative Vehicle-Infrastructure System," *IEEE Transactions on Intelligent Vehicles*, vol. 8, no. 6, pp. 3629–3646, 2023.
- [13] J. Zhou and M. Wang and D. Tian and X. Duan and Y. Shao and Z. Sheng, "Joint Fuel-Efficient Vehicle Platooning and Data Transmission Scheduling for MEC-Enabled Cooperative Vehicle-Infrastructure Systems," *IEEE Transactions on Intelligent Transportation Systems*, vol. 26, no. 2, pp. 2057–2074, 2024.
- [14] J. Mei and K. Zheng and L. Zhao and L. Lei and X. Wang, "Joint Radio Resource Allocation and Control for Vehicle Platooning in LTE-V2V Network," *IEEE Transactions on Vehicular Technology*, vol. 67, no. 12, pp. 12218–12230, 2018.
- [15] T. Zeng and O. Semiari and W. Saad and M. Bennis, "Joint Communication and Control for Wireless Autonomous Vehicular Platoon Systems," *IEEE Transactions on Communications*, vol. 67, no. 11, pp. 7907–7922, 2019.
- [16] C. Hong and H. Shan and M. Song and W. Zhuang and Z. Xiang and Y. Wu, "A Joint Design of Platoon Communication and Control Based on LTE-V2V," *IEEE Transactions on Vehicular Technology*, vol. 69, no. 12, pp. 15893–15907, 2020.
- [17] A. Haraldsen and M. S. Wiig and A. D. Ames and K. Y. Pattersen, "Safety-Critical Control of Nonholonomic Vehicles in Dynamic Environments Using Velocity Obstacles," in *2024 American Control Conference (ACC)*, IEEE, 2024, pp. 3152–3159.
- [18] M. Black and M. Jankovic and A. Sharma and D. Panagou, "Future-Focused Control Barrier Functions for Autonomous Vehicle Control," in *2023 American Control Conference (ACC)*, IEEE, pp. 3324–3331, 2023.
- [19] Y. Xu and J. Zha and J. Ren and X. Jiang and H. Zhang and X. Chen, "Scalable Multi-Agent Reinforcement Learning for Effective UAV Scheduling in Multi-Hop Emergency Networks," in *Proceedings of the 30th Annual International Conference on Mobile Computing and Networking (ACM MobiCom)*, 2024, pp. 2028–2033.
- [20] Y. Zhu and S. B. Andersson, "Safety Guaranteed Optimal Control Policy for Multi-agent Data Harvesting using a CLF-CBF approach," in *2023 American Control Conference (ACC)*, IEEE, 2023, pp. 2123–2128.
- [21] Y. Bian and X. Wang and Y. Tan and M. Hu, C. Du and Z. Sun, "Distributed Model Predictive Control of Connected and Automated Vehicles With Markov Packet Loss," *IEEE Transactions on Transportation Electrification*, vol. 11, no. 2, pp. 6368–6379, 2025.
- [22] N. Keshari and D. Singh, "TCV-D: : An Approach for Path Selection in Vehicular Task Offloading," *Vehicular Communications*, Vol. 47, 2024, 100700.
- [23] Y. Bian and X. Wang and Y. Tan and M. Hu, C. Du and Z. Sun, "Distributed Model Predictive Control of Connected and Automated Vehicles With Markov Packet Loss," *IEEE Transactions on Transportation Electrification*, vol. 11, no. 2, pp. 6368–6379, 2025.
- [24] C. Tsanikidis and J. Ghaderi, "Scheduling Stochastic Traffic With End-to-End Deadlines in Multi-hop Wireless Networks," in *IEEE Conference on Computer Communications, Vancouver (INFOCOM)*, IEEE, 2024, pp. 651–660.
- [25] Kalyanmoy Deb. *Multi-Objective Optimization Using Evolutionary Algorithms*. Wiley Press. 2001.
- [26] S. Song and M. Fan, "Emergency Routing Protocol for Intelligent Transportation Systems Using IoT and Generative Artificial Intelligence," *IEEE Transactions on Intelligent Transportation Systems (Early Access)*, [Online]. Available: doi: 10.1109/TITS.2025.3546340.
- [27] C. Tang and J. Ding and L. Zhang, "LEO Satellite Downlink Distributed Jamming Optimization Method Using a Non-Dominated Sorting Genetic Algorithm," *Remote Sensing*, 2024, 16, 1006.
- [28] Sisi Shi and Xinyan Zhang and Zhihao Wang, "An Improved NSGA-II Algorithm Based on DCD and a-tDX," *Computer Simulation*, 2019, vol. 36, no. 12, pp: 257–262.
- [29] Jian Gong and Carlos Murguia and Anggera Bayuwindra and Jinde Cao, "Resilient Controller Synthesis Against DoS Attacks for Vehicular Platooning in Spatial Domain" in *arXiv:2307.15874*.